Stabilization of Nonclassical States of the Radiation Field in a Cavity by Reservoir Engineering

A. Sarlette,[1,*] J. M. Raimond,[2] M. Brune,[2] and P. Rouchon[3]

[1]*Systems & Modeling, Université de Liège, B28, 4000 Liège Sart-Tilman, Belgium*
[2]*Laboratoire Kastler-Brossel, ENS, UMPC-Paris 6, CNRS, 24 rue Lhomond, 75005 Paris, France*
[3]*Centre Automatique et Systèmes, Mines ParisTech, 60 boulevard Saint Michel, 75006 Paris, France*

(Received 20 November 2010; published 1 July 2011)

We propose an engineered reservoir inducing the relaxation of a cavity field towards nonclassical states. It is made up of two-level atoms crossing the cavity one at a time. Each atom-cavity interaction is first dispersive, then resonant, then dispersive again. The reservoir pointer states are those produced by an effective Kerr Hamiltonian acting on a coherent field. We thereby stabilize squeezed states and quantum superpositions of multiple coherent components in a cavity having a finite damping time. This robust decoherence protection method could be implemented in state-of-the-art experiments.

DOI: 10.1103/PhysRevLett.107.010402 PACS numbers: 03.65.Yz, 03.67.Pp, 42.50.Pq

Nonclassical states of the radiation field are the focus of considerable interest. Squeezed states (SS), with reduced fluctuations on one field quadrature, are interesting for high precision quantum measurements [1]. Mesoscopic field state superpositions (MFSS), involving coherent components with different classical properties, are reminiscent of the famous Schrödinger cat [2], in a superposition of the ''dead'' and ''alive'' states. Their environment-induced decoherence sheds light on the quantum-classical boundary [3]. We envision in this Letter a reservoir engineering setup in cavity quantum electrodynamics (CQED) to generate such states from any initial state and stabilize them.

Many experiments on MFSS have been proposed or realized, particularly with trapped ions [4] (whose harmonic motion is equivalent to a field mode) or CQED [3], with a single atom coupled to a single field mode. Introducing the atom in a state superposition and finally detecting it prepares from a coherent state a MFSS conditioned by the atomic detection outcome [3,5–11].

Deterministic preparation of MFSS could, in principle, be achieved by propagation of an initial coherent field in a Kerr medium [12], described by the Hamiltonian

$$H_K = \zeta_K \mathbf{N} + \gamma_K \mathbf{N}^2 \tag{1}$$

($\mathbf{N}$ is the photon number operator, ζ_K is proportional to the linear index, γ_K is the Kerr frequency; units are chosen such that $\hbar = 1$ throughout the Letter). An initial coherent state $|\alpha\rangle$ evolves with interaction time t_K through nonclassical states $e^{-it_K H_K}|\alpha\rangle$ of mean photon number $|\alpha|^2$ [[3], Section 7.2]. For $t_K\gamma_K \ll \pi$, the field is in a quadrature-squeezed state $|s_\alpha\rangle$ with a nearly Gaussian Wigner function W. For slightly larger interaction times, the field has a ''banana''-shaped Wigner function. For $t_K\gamma_K = \pi/k$, we get a MFSS $|k_\alpha\rangle$ of k equally spaced coherent components [13]. For $t_K\gamma_K = \pi/2$, a MFSS $|c_\alpha\rangle = (|\alpha e^{-i\varphi}\rangle + i|-\alpha e^{-i\varphi}\rangle)/\sqrt{2}$ is reached ($\varphi = \zeta_K t_K$). Note that the collisional interaction Hamiltonian for an atomic sample in a tightly confining potential or in an optical lattice is similar to H_K [14].

The unconditional preparation, protection and long-term stabilization of SS and MFSS is an essential goal for their study and practical use. Reservoir engineering [15,16] protects target quantum states by coupling the system to an ''engineered'' bath whose pointer states (stable states of the system coupled to the reservoir) [17] include the target. The system is effectively decoupled from its standard environment by its much stronger coupling with the engineered bath.

For trapped ions, reservoirs composed of laser fields stabilize a subspace containing superpositions of coherent vibrations [11,15]. However, they do not prevent mixing of states belonging to the stabilized subspace, making it impossible to protect a specific MFSS [[3], p. 487]. A complex reservoir could stabilize a superposition of n phonon number states using $n+2$ lasers [16]. In CQED proposals, reservoirs protect squeezed states [18] and entanglement of two field modes [19]. In [20], a reservoir made up of a stream of atoms crossing the cavity stabilizes MFSS (cotangent states). However, the scheme builds on the fragile trapping state condition [21] (a resonant atom entering the cavity in its upper state undergoes a $2p\pi$ quantum Rabi pulse—p arbitrary integer—in an n-photon field) and state protection is jeopardized by thermal excitation of the cavity at finite temperature.

We propose a robust method to stabilize SS and MFSS in a realistic CQED experiment. It uses an engineered reservoir made up of a stream of 2-level atoms undergoing a tailored composite interaction with the field, dispersive, then resonant, then dispersive again. The reservoir pointer states are then $\approx e^{-it_K H_K}|\alpha\rangle$, in which α and $\gamma_K t_K$ can be chosen at will. We stabilize, in particular, the states $|s_\alpha\rangle$, $|k_\alpha\rangle$ and $|c_\alpha\rangle$.

The method is quite general. Its main idea—combining resonant and dispersive interactions—could be applied to cavity and circuit QED, which can operate in similar regimes. For the sake of definiteness, we discuss it in the context of the ENS CQED setup (Fig. 1, details in [3,7] and below). A microwave field at frequency $\omega_c/2\pi$ is trapped in the cavity C. Atoms are sent one after the other through C. The transition frequency between the atomic lower and upper circular Rydberg states ($|g\rangle$ and $|e\rangle$ respectively) is $\omega_0/2\pi$. The atom-cavity detuning $\delta = \omega_0 - \omega_c \ll \omega_c$ can be controlled with a good time resolution via the Stark effect. The atoms are excited in state $|g\rangle$ in B and prepared by a classical microwave pulse in the Ramsey zone R_1 in the initial state $|u_{\rm at}\rangle = \cos(u/2)|g\rangle + \sin(u/2)|e\rangle$ (without loss of generality, we take phase references so that $\langle g|u_{\rm at}\rangle$ and $\langle e|u_{\rm at}\rangle$ are both real). On a Bloch sphere with $|e\rangle$ at the north pole, it corresponds to a vector at an angle u with the north-south vertical axis. For the engineered reservoir, the final atomic state is irrelevant. Ramsey zone R_2 and the state-selective detector D are used to reconstruct the field state generated by the engineered reservoir, using a method described in [7].

Atom-cavity interaction is ruled by the Jaynes-Cummings Hamiltonian $H_{\rm JC}$. In a proper interaction representation ($\mathbf{a}$: photon annihilation operator):

$$H_{\rm JC} = \frac{\delta}{2}(|e\rangle\langle e| - |g\rangle\langle g|) + i\frac{\Omega(t)}{2}(|g\rangle\langle e|\mathbf{a}^\dagger - |e\rangle\langle g|\mathbf{a}), \quad (2)$$

where $\Omega(t)$ is the atom-cavity coupling, varying with time during the atomic transit through the Gaussian mode. The unitary evolution operators corresponding to resonant ($\delta = 0$) and strongly dispersive ($|\delta| \gg \Omega$) interactions are, within irrelevant phases [3]:

$$U_r(\Theta) = |g\rangle\langle g|\cos(\Theta\sqrt{\mathbf{N}}/2) + |e\rangle\langle e|\cos(\Theta\sqrt{\mathbf{N}+\mathbb{1}}/2) - |e\rangle\langle g|\mathbf{a}\frac{\sin(\Theta\sqrt{\mathbf{N}}/2)}{\sqrt{\mathbf{N}}} + |g\rangle\langle e|\frac{\sin(\Theta\sqrt{\mathbf{N}}/2)}{\sqrt{\mathbf{N}}}\mathbf{a}^\dagger, \quad (3)$$

$$U_d(\phi_0) \approx |g\rangle\langle g|e^{-i\phi_0\mathbf{N}} + |e\rangle\langle e|e^{+i\phi_0(\mathbf{N}+\mathbb{1})}, \quad (4)$$

where $\mathbf{N} = a^\dagger a$ in the functions' arguments is the photon number operator and $\mathbb{1}$ the identity operator; $\Theta = \int\Omega(t)dt$ is the quantum Rabi pulsation in vacuum integrated over time during resonant interaction and $\phi_0 = -(1/4\delta)\int\Omega^2(t)dt$ is the total field phase shift produced by the atom during dispersive interaction.

Resonant atoms initially in $|g\rangle$ absorb photons. The reservoir's pointer state is then the vacuum $|0\rangle$. Resonant atoms initially in $|u_{\rm at}\rangle$ realize a "micromaser" with coherent injection [20,22]. Noticeably, when pumped below population inversion ($0 < u \ll 1$), with $\Theta \ll 1$, this maser stabilizes a coherent state $|\alpha\rangle$. Starting, e.g., from $|0\rangle$ in an ideal cavity, repeated atomic emissions produce a coherent state with a growing real amplitude β. The atoms then undergo a coherent resonant Rabi rotation in this field, with a Bloch vector starting initially towards the south pole. Assuming $\Theta \ll u$, the atomic Bloch vector rotates under $U_r(\Theta)$ by an angle $-\Theta\beta$. For $\Theta\beta < 2u$, the atomic energy decreases on the average and β grows. When β reaches $\alpha = 2u/\Theta$, the average atomic energy is unchanged after interaction and the field amplitude remains constant as an equilibrium is reached. This intuition is supported by developing to second order in u, $\Theta \ll 1$ the master equation for the coarse-grained average of the field density operator map $\rho \to {\rm Tr}_{\rm at}[U_r(\Theta)(\rho \otimes |u_{\rm at}\rangle\langle u_{\rm at}|)U_r(\Theta)^\dagger]$ [23]: the atoms act on the field approximately like a coherent injection plus damping. Numerical simulations show that even for u, $\Theta \approx 1$ the field rapidly converges from any initial state towards a pure state close to $|\alpha\rangle$ with $\alpha \approx 2u/\Theta$.

Our reservoir uses atoms undergoing a composite interaction with the cavity, made up of two opposite dispersive interactions $U_d(\phi_0)$ and $U_d(-\phi_0)$ sandwiching $U_r(\Theta)$. The composite evolution operator is $U_c = U_d(\phi_0)U_r(\Theta)U_d^\dagger(\phi_0)$. Using $\mathbf{a}f(\mathbf{N}) = f(\mathbf{N}+\mathbb{1})\mathbf{a}$, we get

$$U_c = |g\rangle\langle g|\cos(\Theta\sqrt{\mathbf{N}}/2) + |e\rangle\langle e|\cos(\Theta\sqrt{\mathbf{N}+\mathbb{1}}/2) - |e\rangle\langle g|\mathbf{a}\frac{\sin(\Theta\sqrt{\mathbf{N}}/2)}{\sqrt{\mathbf{N}}}e^{2i\phi_0\mathbf{N}} + |g\rangle\langle e|\frac{\sin(\Theta\sqrt{\mathbf{N}}/2)}{\sqrt{\mathbf{N}}}e^{-2i\phi_0\mathbf{N}}\mathbf{a}^\dagger. \quad (5)$$

When the atom remains in the same state, the dispersive interactions cancel. When it switches level in $U_r(\Theta)$, the dispersive phase shifts add up. In semiclassical terms, an atomic absorption (emission) decreases (increases) the field amplitude and increases (decreases) its phase. After many atomic interactions, a larger field is expected to have a smaller accumulated phase than a smaller field, in close analogy with the Kerr effect action.

Observing that $e^{-i\phi_0\mathbf{N}(\mathbf{N}+\mathbb{1})}\mathbf{a}e^{i\phi_0\mathbf{N}(\mathbf{N}+\mathbb{1})} = \mathbf{a}e^{2i\phi_0\mathbf{N}}$, U_c can be rewritten as:

$$U_c = \exp[-ih_0(\mathbf{N})]U_r(\Theta)\exp[ih_0(\mathbf{N})],$$

with $h_0(\mathbf{N}) = \phi_0\mathbf{N}(\mathbf{N}+\mathbb{1})$. The pointer state of the composite reservoir U_c is thus deduced from that of the resonant reservoir U_r by a basis change described by the unitary $\exp[-ih_0(\mathbf{N})]$. Since $h_0(\mathbf{N}) = H_K t_K$ for $\gamma_K t_K = \zeta_K t_K = \phi_0$, this basis change is equivalent to the action of a Kerr medium. The composite interaction reservoir can thus stabilize any state of the type $\exp[-iH_K t_K]|\alpha\rangle$, with t_K chosen by adjusting the interaction parameters. In particular, for $\phi_0 = \pi/2$, we stabilize up to an irrelevant phase the MFSS $|c_\alpha\rangle = (|-i\alpha\rangle + i|i\alpha\rangle)/\sqrt{2}$.

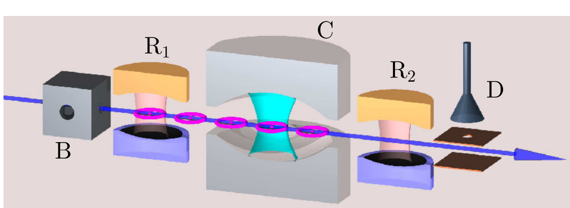

FIG. 1 (color online). Scheme of the ENS CQED experiment.

Let us give an intuitive insight into the stabilization of $|c_\alpha\rangle$. Assume that, before interacting with an atom, the field is in the state $|\psi_0\rangle = (|-i\alpha_0\rangle + i|i\alpha_0\rangle)/\sqrt{2}$ with $\alpha_0 < \alpha$ [24]. The first dispersive interaction entangles atom and field in a mesoscopic quantum superposition, correlating two π-phase shifted atomic dipoles $|u_{\rm at}\rangle$ and $|(-u)_{\rm at}\rangle$ with coherent states $|\alpha_0\rangle$ and $|-\alpha_0\rangle$ respectively. As explained above, during the resonant interaction each dipole state amplifies the correlated coherent component from $\pm\alpha_0$ to $\pm\tilde{\alpha}$ ($\alpha_0 < \tilde{\alpha} < \alpha$). The second dispersive interaction disentangles atom and field. The final field state is thus independent upon the atomic one and writes $|\psi_t\rangle = (|-i\tilde{\alpha}\rangle + i|i\tilde{\alpha}\rangle)/\sqrt{2}$, a "larger" MFSS. Similarly, if $\alpha_0 > \alpha$, the atomic interaction reduces the MFSS amplitude. Altogether, the atoms stabilize a sizable MFSS.

Equation (4) is valid in the large detuning limit. For smaller δ values, of the order of the maximum atom-field coupling, a more complex expression with the full dressed states should be used, reflecting a finite transition probability between atomic levels during dispersive interaction. Further analysis [23] and numerical simulations of the exact dynamics surprisingly show that our main findings remain quite valid even in this regime. The reservoir's pointer state is still that produced by a Kerr hamiltonian acting onto a coherent state close to $|\alpha\rangle$.

We have performed numerical simulations of the field evolution in realistic experimental conditions, corresponding to the present ENS CQED setup (Fig. 1). The cavity and atomic frequencies are close to 51 GHz, corresponding to the transition between circular rubidium Rydberg levels with principal quantum numbers 51 and 50. Taking the origin of time when the atom crosses cavity axis, $\Omega(t) = \Omega_0 e^{-v^2t^2/w^2}$ in the Gaussian mode of C, where v is the adjustable atomic velocity, $\Omega_0/2\pi = 50$ kHz and $w = 6$ mm. The simulations take into account the standard cavity relaxation towards thermal equilibrium. The photon lifetime in C is $T_c = 65$ ms (value for the present ENS cavity) and the residual thermal field at the mirrors' temperature (0.8 K) corresponds to a mean number of blackbody photons per mode $n_t = 0.05$. The engineered reservoir is meant to protect nonclassical states from this decoherence.

The composite atom-field interaction is achieved with a ladder of Stark shifts during atom-cavity interaction. The corresponding evolution operators are computed exactly from $H_{\rm JC}$ [Eq. (2)] using the quantum optics package for MATLAB [25] (Hilbert space is truncated to the 60 first Fock states). Atom-field interaction is supposed to start when $vt = -1.5w$ (dispersive coupling equal to $\sim 1\%$ of its maximum value) and ends when $vt = 1.5w$, the total interaction time being $t_i = 3w/v$. During t_i, δ is first set at $\delta = \Delta > 0$, implementing $U_d^\dagger$, then at $\delta = 0$ for a short time span t_r centered on cavity center crossing time, and finally $\delta = -\Delta$ for U_d.

Atomic samples are produced at regular time intervals in B. The probability for having one atom in a sample, $p_{\rm at} \simeq 0.3$, is kept low to avoid having two atoms at a time in C. Interaction with the next sample starts just after the previous one has left C. So smaller t_i implies more frequent atom-cavity interaction, i.e., a stronger engineered reservoir to counteract standard cavity relaxation. We trace over the irrelevant final atomic state to compute the field density matrix ρ after each atomic interaction.

Figure 2(a) presents the experimentally accessible [7] Wigner function $W(\xi)$ associated to the cavity field state ρ_{200} after its interaction with 200 atomic samples for $v = 70$ m/s (requiring a moderate laser cooling of the rubidium atomic beam), $t_i = 257$ μs, $\Delta = 2.2\Omega_0$, $t_r = 5$ μs, $\Theta \approx \pi/2$, $u = 0.45\pi$. The (irrelevant) initial cavity state is the vacuum. We get a two-component MFSS with strong negativities in W. The average photon number is $\bar{n} = 2.72$. This corresponds to a MFSS "size" (square of the distance between components in the phase space) of 10.9, comparable to that achieved in [7].

The purity $P = {\rm Tr}(\rho_{200}^2)$ is 51%. We estimate the fidelity $F = {\rm Tr}[\rho_{200}\rho_{c_\alpha}]$ of this state with respect to a MFSS ρ_{c_α} of two coherent states with opposite phases, optimized by adjusting in the reference state the phase and amplitude of the coherent components and their relative quantum phase. We get $F = 69\%$. We have checked that cavity relaxation

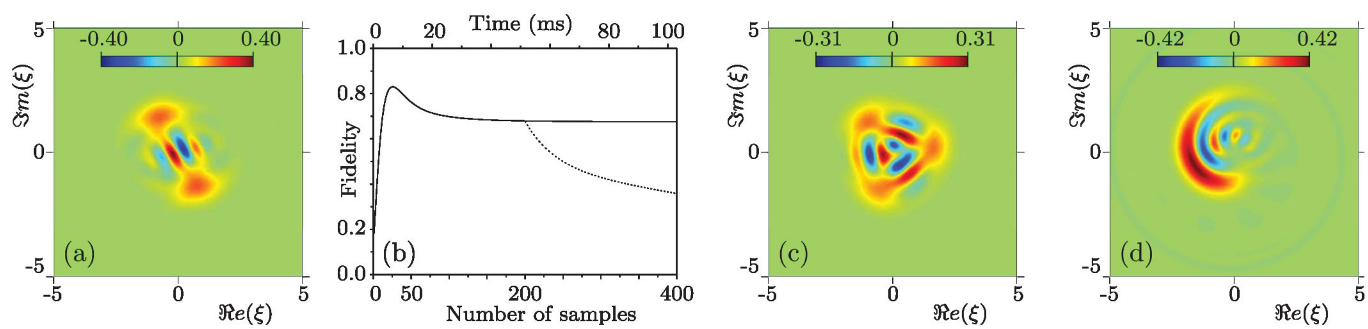

FIG. 2 (color). Nonclassical states stabilized by the engineered reservoir. (a) Wigner function of the cavity field after 200 steps of reservoir-atom interaction. The state is close to $|c_\alpha\rangle$. (b) Solid line: fidelity of the generated state against the closest $|c_\alpha\rangle$ as a function of number of interactions (bottom axis) or of time (upper axis). Dashed line: reservoir is switched off after 200 interactions. (c) and (d) Wigner functions of stabilized cavity fields close to $|k_\alpha\rangle$ with $k = 3$ and to a "banana state", respectively. Detailed conditions in the text.

is the main cause of imperfection, F being 98% in an ideal cavity.

Figure 2(b) presents as a solid line the fidelity F of the prepared state w.r.t. the final ideal MFSS as a function of atomic sample number (i.e., as a function of time). The transient reflects the competition between the fast buildup of the MFSS, the fidelity raising over a few atomic samples only, and the MFSS decoherence, whose time scale $T_d = T_c/(2\bar{n})$ [3,7] becomes relevant once a large average photon number $\bar{n}$ has been produced. The steady state fidelity is reached after $\simeq 100$ samples. The dashed line presents F when we switch off the reservoir after 200 interactions. It initially drops much more rapidly than $T_c = 65$ ms, illustrating the high sensitivity of the generated nonclassical state to decoherence and its efficient protection by the engineered reservoir.

For a slightly larger detuning, $\Delta = 3.7\Omega_0$ (all other parameters unchanged), we obtain a three-component MFSS $|k_\alpha\rangle$ with $k = 3$ [Fig. 2(c)], $\bar{n} = 2.70$ photons, $P = 56\%$, and a fidelity with respect to the closest three-component ideal MFSS $F = 73\%$.

In the Kerr dynamics, squeezed states are obtained in the early stages of the initial coherent state phase spreading. With $v = 300$ m/s, $t_i = 60$ μs, $t_r = 1.7$ μs i.e. $\Theta \approx 0.17\pi$, $u = \pi/2$ and $\Delta = 70\Omega_0$, we generate after 200 samples a Gaussian minimal uncertainty state for the Heisenberg relations between orthogonal field quadratures containing $\bar{n} = 21$ photons, with a 1.5 dB squeezing.

For larger Kerr-induced phase spreads, the Wigner function takes a banana shape, with nonminimal uncertainty but nonclassical Wigner function negativities. As an example, Fig. 2(d) presents the Wigner function of the field obtained after 200 samples with $v = 150$ m/s, $t_i = 120$ μs, $t_r = 5$ μs i.e. $\Theta \approx \pi/2$, $u = \pi/2$ and $\Delta = 7\Omega_0$. The field has $\bar{n} = 3.52$ and $P = 91\%$.

All these settings are within reach of the present ENS setup with the addition of a moderate atomic beam laser cooling to achieve proper velocities. The attainable photon number in the pointer states will result from a compromise between cavity decoherence and reservoir efficiency. States corresponding to low ϕ_0 values are more efficiently stabilized since they allow faster, thus more frequent, atoms and they are less affected by relaxation. MFSS with 3 or 4 components and a photon number in the 3-6 range are accessible. We have checked that the scheme is not sensitive to experimental imperfections (a few percent variation of the interaction parameters does not appreciably modify the steady state), as long as the symmetry between the two dispersive interactions is accurate. A more detailed discussion will be published elsewhere [23].

In conclusion, we have shown that composite atom-cavity interactions allow us to engineer an environment driving a cavity field deterministically towards nonclassical field states including the Schrödinger-cat-like mesoscopic field state superpositions. A key feature of the engineered reservoir with respect to other nonclassical states generation techniques [3,5–11] is that it drives any initial cavity state to the target state and stabilizes this quantum resource for arbitrarily long times. It does not require recording the final atomic states, unlike quantum feedback experiments, which can also stabilize nonclassical states [26]. The scheme is simple and robust enough to be amenable to experiment in a state-of-the-art CQED setup.

The authors thank I. Dotsenko, S. Gleyzes, S. Haroche, and M. Mirrahimi for enlightening discussions and references. A. S. acknowledges FNRS, Mines ParisTech and the IAP (DYSCO). J. M. R. and M. B. acknowledge support of the EU and ERC (AQUTE and DECLIC projects) and from the ANR (QUSCO-INCA). P. R. acknowledges support from ANR (CQUID).

*alain.sarlette@ulg.ac.be

[1] C. M. Caves, Phys. Rev. D **23**, 1693 (1981); J. P. Dowling, Contemp. Phys. **49**, 125 (2008).
[2] E. Schrödinger, Naturwissenschaften **23**, 807 (1935).
[3] S. Haroche and J.-M. Raimond, *Exploring the Quantum: Atoms, Cavities and Photons* (Oxford University Press, Oxford, 2006).
[4] C. Monroe *et al.*, Science **272**, 1131 (1996); C. J. Myatt *et al.*, Nature (London) **403**, 269 (2000).
[5] M. Brune *et al.*, Phys. Rev. A **45**, 5193 (1992).
[6] M. Brune *et al.*, Phys. Rev. Lett. **77**, 4887 (1996).
[7] S. Deléglise *et al.*, Nature (London) **455**, 510 (2008).
[8] L. Davidovich *et al.*, Phys. Rev. Lett. **71**, 2360 (1993).
[9] C. J. Villas-Bôas *et al.*, J. Opt. B **5**, 391 (2003).
[10] E. Solano, G. S. Agarwal, and H. Walther, Phys. Rev. Lett. **90**, 027903 (2003).
[11] R. L. de Matos Filho and W. Vogel, Phys. Rev. Lett. **76**, 608 (1996).
[12] B. Yurke and D. Stoler, Phys. Rev. Lett. **57**, 13 (1986).
[13] The components are well separated only in the case $k < \pi\alpha$ ([3], Section 7.2).
[14] S. Will *et al.*, Nature (London) **465**, 197 (2010).
[15] J. F. Poyatos, J. I. Cirac, and P. Zoller, Phys. Rev. Lett. **77**, 4728 (1996).
[16] A. R. R. Carvalho *et al.*, Phys. Rev. Lett. **86**, 4988 (2001).
[17] W. H. Zurek, Phys. Rev. D **24**, 1516 (1981).
[18] T. Werlang *et al.*, Phys. Rev. A **78**, 033820 (2008).
[19] S. Pielawa *et al.*, Phys. Rev. Lett. **98**, 240401 (2007).
[20] J. J. Slosser, P. Meystre, and S. L. Braunstein, Phys. Rev. Lett. **63**, 934 (1989).
[21] P. Filipovicz, J. Javanainen, and P. Meystre, J. Opt. Soc. Am. B **3**, 906 (1986).
[22] F. Casagrande, A. Lulli, and V. Santagostino, Phys. Rev. A **65**, 023809 (2002).
[23] A. Sarlette *et al.* (to be published).
[24] This restriction is only for interpretation: the reservoir drives any initial state to the desired cat.
[25] S. M. Tan, J. Opt. B **1**, 424 (1999).
[26] I. Dotsenko *et al.*, Phys. Rev. A **80**, 013805 (2009).